Seismic interferometry: a comparison of approaches

Kees Wapenaar, Deyan Draganov, Joost van der Neut and Jan Thorbecke, Delft University of Technology

Summary We discuss three approaches to seismic interferometry and compare their underlying assumptions. In the first approach the reflection response is reconstructed by cross-correlating the responses of many uncorrelated noise sources. In the second approach a depth image is obtained from the response of a single source, recorded by many receivers. In the third approach the Green's function is reconstructed by cross-correlating the recordings of two receivers in a diffuse field.

Introduction

Seismic interferometry is the process of cross-correlating seismic traces recorded at different locations at the Earth's surface with the aim of retrieving information about the subsurface (Schuster et al., 2003). An early contribution is Claerbout's work on the synthesis of a layered medium from its acoustic transmission response (Claerbout, 1968). He showed that the autocorrelation of the transmission response of a horizontally layered medium, bounded by a free surface, yields the reflection response of this medium. Later he conjectured for 3-D media that the cross-correlation of the transmission response observed at different locations gives the reflection response that would be recorded at one of the locations if there was a source at the other. This conjecture was confirmed by numerical experiments (Rickett and Claerbout, 1996), explained with stationary phase arguments (Schuster, 2001) and proven to be correct under specific assumptions (Wapenaar et al., 2002).

Independently, another approach to reconstruct reflection responses from cross-correlations was introduced by Lobkis and Weaver (2001). They showed that the Green's function of a medium emerges by cross-correlating the recordings of two receivers in a diffuse field. Campillo and Paul (2003) used this approach to reconstruct surface wave responses between two stations from recordings of distant earthquakes. Malcolm et al. (2003) demonstrated the validity of this approach with ultrasonic laboratory measurements in highly heterogeneous rock.

In this paper we briefly review the approaches mentioned above and discuss their underlying assumptions. The discussion will be rather intuitive; for more precise derivations we refer to the papers mentioned above. In the examples we consider buried noise sources in the subsurface; however, most conclusions also apply to situations where the sources are located at the surface.

Essentials of seismic interferometry

Following Schuster (2001), the essentials of seismic interferometry can be explained with the example shown in Figures 1 and 2. A source, buried in the subsurface at $\mathbf{x}_S$, emits a noise signal to the surface, where it is recorded at $\mathbf{x}_A$ (the first trace in Figure 2). At the surface it gets reflected, after which it propagates downward, gets scattered by the diffractor at $\mathbf{x}_D$ and propagates again to the surface where it is recorded at $\mathbf{x}_B$ (the second trace in Figure 2). The time-delay between these two signals (t_{AB} in Figure 2) is equal to the propagation time from $\mathbf{x}_A$ via the diffractor at $\mathbf{x}_D$ to $\mathbf{x}_B$. Hence, the cross-correlation of the two signals (the third trace in Figure 2), which shows a (band-limited) impulse at t_{AB}, can be interpreted as the reflection response that would be measured at $\mathbf{x}_B$ if there was a source at $\mathbf{x}_A$. Of course this example is oversimplified. We have assumed that at $\mathbf{x}_A$ we only recorded the direct arrival and at $\mathbf{x}_B$ only the scattered wave field. Furthermore, we considered only a single diffractor and we ignored higher order reflections. Last, but not least, we assumed that one of the traces is recorded exactly at the specular point $\mathbf{x}_A$ where the signal is reflected downward into the subsurface. In the following we show how the methods discussed in the introduction get around these assumptions.

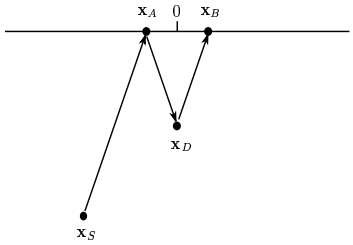

Fig. 1: Configuration for seismic interferometry example. The propagation velocity is $c = 1500$ m/s. Furthermore, $\mathbf{x}_A = (-100, 0)$, $\mathbf{x}_B = (100, 0)$, $\mathbf{x}_S = (-300, 600)$ and $\mathbf{x}_D = (0, 300)$.

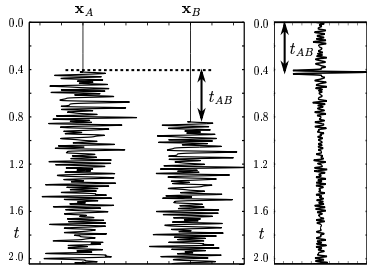

Fig. 2: Direct arrival at $\mathbf{x}_A$, scattered arrival at $\mathbf{x}_B$ and their cross-correlation, which simulates the reflection response.

1. Interferometry with multiple sources

Consider the situation depicted in Figure 3, in which there are multiple noise sources buried in the subsurface. The

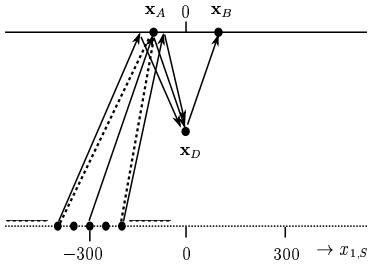

Fig. 3: Seismic interferometry with multiple sources.

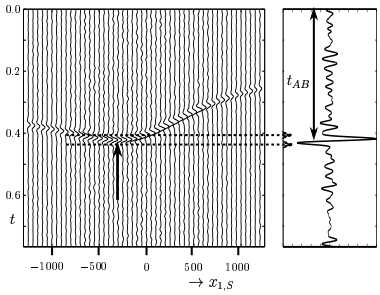

Fig. 4: Cross-correlation results for all source positions (left) and their sum (right) which simulates the reflection response.

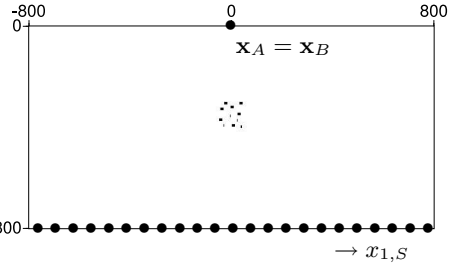

Fig. 5: Seismic interferometry with multiple sources: numerical example with cluster of 10 diffractors.

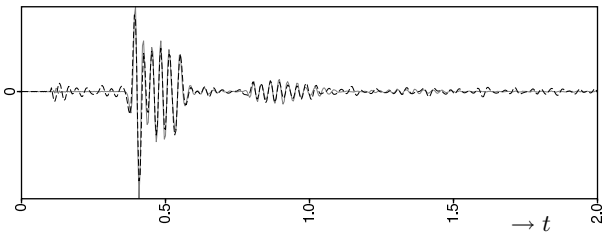

Fig. 6: Reconstructed reflection response (dashed black) obtained by correlation of transmission responses and directly modelled reflection response (solid grey).

source at $x_{1,S} = -300$ is the one we considered in the previous example. The ray that leaves this source reflects at $\mathbf{x}_A$ on its way to the diffractor and $\mathbf{x}_B$. The rays leaving the other sources have their specular reflection points left and right from $\mathbf{x}_A$ (the solid rays in Figure 3). The direct arrivals at $\mathbf{x}_A$ follow the dashed paths and do not coincide with the solid rays, except for the source at $x_{1,S} = -300$. For each of the sources we cross-correlate the direct arrival at $\mathbf{x}_A$ with the scattered wave recorded at $\mathbf{x}_B$. The correlation results are shown in Figure 4, in which the horizontal axis denotes the source coordinate $x_{1,S}$. The trace at $x_{1,S} = -300$ shows again an impulse at t_{AB}, similar as in the previous example; the impulses in the surrounding traces arrive before t_{AB}. If we sum the traces for all $x_{1,S}$ the main contribution comes from an area (the Fresnel zone) around the point $x_{1,S} = -300$ where the arrival times are stationary (denoted by the vertical arrow); the other contributions more or less cancel. Hence, the summed result, shown in the right frame in Figure 4, contains an impulse at t_{AB} and can again be interpreted as the reflection response that would be measured at $\mathbf{x}_B$ if there was a source at $\mathbf{x}_A$. Note that this procedure works for any $\mathbf{x}_A$ and $\mathbf{x}_B$, as long as the array of sources contains a source that emits a specular ray via $\mathbf{x}_A$ and the diffractor to $\mathbf{x}_B$.

What we have just presented is an intuitive justification of the following equation

$$\int_{\partial\mathcal{D}_m} T^-(\mathbf{x}_A, \mathbf{x}, -t) * T^-(\mathbf{x}_B, \mathbf{x}, t) \mathrm{d}^2\mathbf{x} = \tag{1}$$
$$\delta(\mathbf{x}_{H,B} - \mathbf{x}_{H,A})\delta(t) - R^+(\mathbf{x}_B, \mathbf{x}_A, -t) - R^+(\mathbf{x}_B, \mathbf{x}_A, t)$$

(Wapenaar et al., 2002), where $*$ denotes temporal convolution and $\mathbf{x}_H = (x_1, x_2)$ represents the horizontal coordinate vector. The integrand in the left-hand side contains the cross-correlation of upgoing transmission responses recorded at $\mathbf{x}_A$ and $\mathbf{x}_B$ for a range of sources at $\mathbf{x}$ at some depth level $\partial\mathcal{D}_m$ in the subsurface (the traces in Figure 4); an integral is carried out along these sources at $\partial\mathcal{D}_m$ (the summation in Figure 4). Because the transmission responses contain all arrivals (unlike in the example above), the correlations give a significant contribution at $t = 0$ (represented by the delta function) and at negative times (represented by $R^+(\mathbf{x}_B, \mathbf{x}_A, -t)$). By removing the delta function, setting the non-causal part to zero and changing the sign, what remains is the reflection response $R^+(\mathbf{x}_B, \mathbf{x}_A, t)$. Equation (1) has been derived for an arbitrary lossless inhomogeneous medium between the free surface and the depth level $\partial\mathcal{D}_m$. Hence, the reconstructed reflection response $R^+(\mathbf{x}_B, \mathbf{x}_A, t)$ correctly contains primaries and multiple reflections. We illustrate this for the configuration of Figure 5, which contains a cluster of 10 diffractors in a homogeneous background model with propagation velocity $c = 1500$ m/s. We modelled the transmission responses for a range of noise sources at a depth of 800 m. Using equation (1) we reconstructed the reflection response at $\mathbf{x}_A = \mathbf{x}_B = (0, 0)$, which is represented by the dashed black line in Figure 6. It matches very accurately the directly modelled reflection response, represented by the solid grey line in this figure.

Note that in equation (1) as well as in the examples we assumed that the responses from all sources $\mathbf{x}$ at $\partial\mathcal{D}_m$ have been separately measured. Let us now assume that we measure the responses of all noise sources simultaneously, and call these responses $T^-_{\mathrm{obs}}(\mathbf{x}_A, t)$ and $T^-_{\mathrm{obs}}(\mathbf{x}_B, t)$. Each of these terms is an integral along the sources at $\partial\mathcal{D}_m$. The cross-correlation $T^-_{\mathrm{obs}}(\mathbf{x}_A, -t) * T^-_{\mathrm{obs}}(\mathbf{x}_B, t)$ is

thus a double integral along these sources. However, if we assume these sources are uncorrelated, then this double integral reduces to the single integral in the left-hand side of equation (1). Hence, we finally obtain (for $t > 0$)

$$R^+(\mathbf{x}_B, \mathbf{x}_A, t) = -T^-_{\rm obs}(\mathbf{x}_A, -t) * T^-_{\rm obs}(\mathbf{x}_B, t), \quad (2)$$

where $T^-_{\rm obs}(\mathbf{x}_A, -t) * T^-_{\rm obs}(\mathbf{x}_B, t)$ is simply the cross-correlation of two recordings at $\mathbf{x}_A$ and $\mathbf{x}_B$ at the surface.

2. Interferometry with multiple receivers

Consider the situation depicted in Figure 7, which contains again a single noise source at $\mathbf{x}_S$ in the subsurface, but this time there are multiple receivers at the surface. The receiver at $x_{1,A} = -100$ is the one we considered in the previous examples. It is the specular reflection point for the ray that leaves the source at $\mathbf{x}_S$ and propagates via the free surface to the diffractor at $\mathbf{x}_D$. In principle we could follow the same approach as in the previous section, that is, cross-correlate the direct arrivals at all receivers with the scattered wave recorded at $\mathbf{x}_B$ and sum the results for all $x_{1,A}$. The result would contain an impulse at t_{AB} and could again be interpreted as the reflection response that would be measured at $\mathbf{x}_B$ if there was a source at $x_{1,A} = -100$. However, this is only useful if we know the position of the specular reflection point. In practice this procedure is useless, since for each diffractor the specular reflection point is different. Also the position of the source is usually unknown.

Schuster (2001), Artman et al. (2004) and Draganov et al. (2004) get around this problem by combining the cross-correlation process with migration (which is also a cross-correlation process). For the configuration in Figure 7 the procedure is as follows. The direct arrivals at $x_{1,A}$ are forward extrapolated to the diffractor at $\mathbf{x}_D$ along the dashed paths in Figure 7. The scattered wave recorded at $\mathbf{x}_B$ is inversely extrapolated along the rightmost dashed path in this figure. These forward and inverse extrapolation results are cross-correlated. The correlation results are shown in Figure 8, in which the horizontal axis denotes the receiver coordinate $x_{1,A}$. The trace at $x_{1,A} = -100$ (the specular reflection point) shows an impulse at $t = 0$; the impulses in the surrounding traces arrive before $t = 0$. The summed result, shown in the right frame in Figure 8, also contains an impulse at $t = 0$. According to the imaging condition in migration, this impulse at $t = 0$ should be positioned at the image point, which in this case corresponds to the diffractor position $\mathbf{x}_D$ (had we chosen another image point at which there is no diffractor, then the summed trace would contain noise at $t = 0$). Note that this procedure works for any $\mathbf{x}_S$ and $\mathbf{x}_D$, as long as the array of receivers includes the specular reflection point.

Schuster calls the combined process described above "interferometric imaging". When there is only one source it is not possible to reconstruct the reflection response $R^+(\mathbf{x}_B, \mathbf{x}_A, t)$ as an intermediate result. Instead, this procedure directly maps the primary reflections to their correct position in depth. When applied in practice, the full transmission responses are involved (instead of only direct arrivals and single scattered waves). This leads to ghost images, similar as in migration of normal surface data, plus a strong event at zero depth, comparable with the delta contribution in the previous section (the latter event can be simply muted). Examples are given by Draganov et al. (2004).

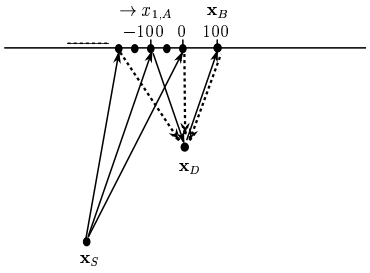

Fig. 7: Seismic interferometry with multiple receivers.

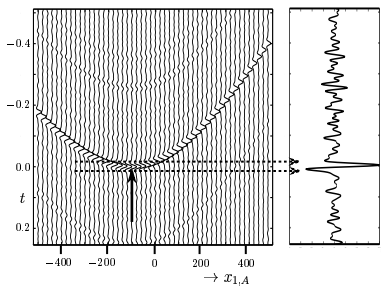

Fig. 8: Cross-correlation results (after forward and inverse extrapolation to $\mathbf{x}_D$) for all receiver positions (left) and their sum (right). The impulse at $t = 0$ is the image at $\mathbf{x}_D$.

3. Interferometry with multiple scatterers

Consider the situation depicted in Figure 9, which contains multiple scatterers and a single transient source at $\mathbf{x}_S$ in the subsurface. We assume again that the medium is lossless. The wave field in this configuration can be written as an integral of weighted eigenfunctions $\phi_\lambda(\mathbf{x})$ of the wave equation (the integral is along the spectrum of eigenvalues λ). Hence, the cross-correlation of two recordings at $\mathbf{x}_A$ and $\mathbf{x}_B$ is a double integral of products of eigenfunctions $\phi_\lambda(\mathbf{x}_A)\phi_\mu(\mathbf{x}_B)$, which reduces to a single integral of $\phi_\lambda(\mathbf{x}_A)\phi_\lambda(\mathbf{x}_B)$ when the wave field is diffuse (again, the integral is along λ). Since the Green's

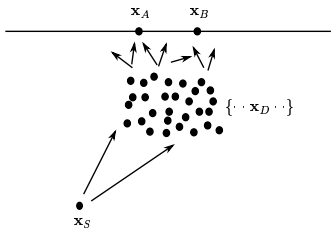

Fig. 9: Seismic interferometry with multiple scatterers.

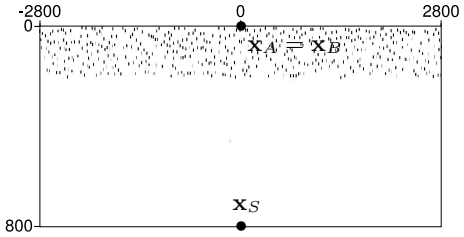

Fig. 10: Seismic interferometry with 500 multiple scatterers: numerical example.

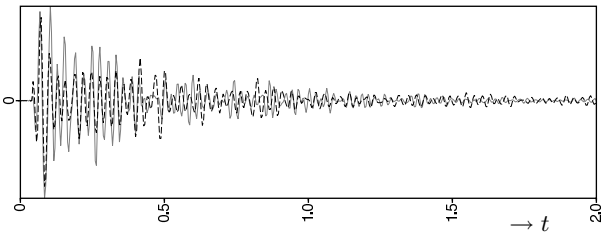

Fig. 11: Reconstructed reflection response (dashed black) obtained by correlation of transmission responses and directly modelled reflection response (solid grey).

function can also be written as a weighted integral of $\phi_\lambda(\mathbf{x}_A)\phi_\lambda(\mathbf{x}_B)$, it thus follows that the cross-correlation of two recordings at $\mathbf{x}_A$ and $\mathbf{x}_B$ is proportional to the Green's function. This is in a nutshell the theory of Lobkis and Weaver (2001). Note that the theory is not restricted to transient sources. Any source signal with an autocorrelation close to an impulse will do.

We illustrate this method for the configuration in Figure 10, which contains 500 randomly placed diffractors in a homogeneous background model with propagation velocity $c = 1500$ m/s. We modelled the transmission response for a single noise source at $\mathbf{x}_S = (0, 800)$. We reconstructed the reflection response at $\mathbf{x}_A = \mathbf{x}_B = (0, 0)$, which is represented by the dashed black line in Figure 11. It reasonably matches the directly modelled reflection response, represented by the solid grey line in this figure.

Discussion

We compare the main underlying assumptions of the different methods of seismic interferometry discussed above.

In all approaches, it is assumed that the medium is lossless. In methods 1 and 3 the full time-dependent reflection response is reconstructed, including multiple reflections, whereas method 2 yields an image in depth, in which only the primaries are correctly mapped. Of course the reconstructed reflection responses of methods 1 and 3 can be mapped into depth as well, see Artman et al. (2004) and Draganov et al. (2004).

Methods 1 and 2 make no assumptions about the complexity of the medium, whereas method 3 assumes that the medium is heterogeneous in such a way that the wave field is diffuse. Criteria for diffuse wave fields in heterogeneous media are discussed by van Wijk and Scales (2002).

Method 1 requires either many subsequent measurements of many source responses (equation 1) or simultaneous measurements of many uncorrelated sources (equation 2). In the latter situation the wave field is again diffuse, but the cause is different from that in method 3 (uncorrelated sources versus uncorrelated medium parameters). Opposed to this, method 2 makes no assumptions about diffusivity at all; a single source in a fully deterministic medium suffices.

The main application of seismic interferometry is in passive seismics. In practice, the conditions for passive seismics will most likely be a combination of the situations described above, i.e., a limited number of uncorrelated noise sources and a limited amount of randomness of the medium parameters. Both conditions contribute to the accuracy of the reconstruction of the reflection response.

References

Artman, B., Draganov, D., Wapenaar, C. P. A., and Biondi, B., 2004, Direct migration of passive seismic data: 66th Mtg., Eur. Assoc. Expl Geophys., Extended Abstracts, Session: P075.

Campillo, M., and Paul, A., 2003, Long-range correlations in the diffuse seismic coda: Science, **299**, 547–549.

Claerbout, J. F., 1968, Synthesis of a layered medium from its acoustic transmission response: Geophysics, **33**, 264–269.

Draganov, D., Wapenaar, C. P. A., Artman, B., and Biondi, B., 2004, Migration methods for passive seismic data: 74th Annual Internat. Mtg., Soc. Expl. Geophys., Expanded Abstracts, (submitted).

Lobkis, O. I., and Weaver, R. L., 2001, On the emergence of the Green's function in the correlations of a diffuse field: J. Acoust. Soc. Am., **110**, 3011–3017.

Malcolm, A. E., Scales, J. A., and van Tiggelen, B. A., 2003, Extracting the Green function from diffuse, equipartitioned waves (submitted and available at http://acoustics.mines.edu).

Rickett, J., and Claerbout, J. F., 1996, Passive seismic imaging applied to synthetic data: Technical report, Stanford Exploration Project.

Schuster, G. T., Yu, J., Sheng, J., and Rickett, J., 2003, Interferometric/Daylight seismic imaging: Geoph. J. Int., (accepted).

Schuster, G. T., 2001, Theory of daylight/interferometric imaging: tutorial: 63rd Mtg., Eur. Assoc. Expl Geophys., Extended Abstracts, Session: A32.

van Wijk, K., and Scales, J. A., 2002, Unknowns in multiple scattering: 64th Mtg., Eur. Assoc. Expl Geophys., Extended Abstracts, Session: C029.

Wapenaar, C. P. A., Draganov, D., Thorbecke, J. W., and Fokkema, J. T., 2002, Theory of acoustic daylight imaging revisited: 72nd Annual Internat. Mtg., Soc. Expl. Geophys., Expanded Abstracts, 2269-2272